Visualization of a functionally enhanced GFP-tagged galanin R2 receptor in PC12 cells: Constitutive and ligand-induced internalization

Sheng Xia*†, Svend Kjær*, Kang Zheng*, Ping-Sheng Hu‡, Li Bai†, Jun-Yong Jia*, Rudolf Rigler§, Aladdin Pramanik§, Tao Xu†, Tomas Hökfelt*, and Zhi-Qing David Xu*§¶‖

Departments of *Neuroscience and §Medical Biochemistry and Biophysics and ¶Center for Genomics and Bioinformatics, Karolinska Institutet, S-171 77 Stockholm, Sweden; †School of Life Science and Technology, Huazhong University of Science and Technology, Wuhan, Hubei 430074, People's Republic of China; and ‡Molecular Pharmacology I, Department of Assay Development and Screening, Biovitrum AB, S-112 76 Stockholm, Sweden

Contributed by Tomas Hökfelt, September 7, 2004

Trafficking of the galanin R2 receptor (GALR2) fused with enhanced GFP (EGFP) was studied by using confocal fluorescence microscopy. The fusion protein was predominantly localized on the plasma membrane with some intracellular fluorescent structures (vesicles), mainly in the perinuclear region. Incubation with galanin resulted in a concentration-dependent increase in intracellular Ca^{2+} concentration levels, suggesting that the GALR2-EGFP conjugate is functional. After blocking endocytosis with methyl-β-cyclodextrin GALR2-EGFP expression was increased on the surface and decreased in the cytoplasm. Blocking endocytic recycling with monensin caused an increase of intracellular GALR2-EGFP accumulation and a decrease of fluorescence on the plasma membrane. GALR2-EGFP on the plasma membrane was internalized within 5–10 min after treatment with galanin or AR-M1896, a selective GALR2 agonist, with a dramatic reduction in plasma membrane localization and appearance in intracellular vesicles. Neither M35 nor M40, two galanin analogues with putative antagonistic action, prevented GALR2 agonist-induced internalization of GALR2-EGFP, suggesting that they are not antagonists at this receptor under the present circumstances. Galanin stimulation at low temperature caused GALR2-EGFP aggregation and clustering on the surface but no translocation to cytoplasm. After coincubation with galanin the GALR2-EGFP was colocalized with internalized Texas red-transferrin, a marker of the clathrin endocytic pathway. Hyperosmotic sucrose inhibited internalization of GALR2-EGFP. Taken together these findings indicate that GALR2 undergoes constitutive endocytosis and recycling and that both ligand-independent and ligand-dependent internalization use the clathrin-dependent endocytic recycling pathway.

Galanin (1), a 29-aa neuropeptide (30 aa in humans), is widely distributed in the nervous system and has been suggested to be involved in numerous neuronal functions, including learning and memory, pain, and feeding behaviors (reviewed in ref. 2), and to exert trophic effects (3). In the locus coeruleus and dorsal raphe of rats galanin reduces firing rate and induces hyperpolarization with a marked desensitization (4–7). So far, three receptor subtypes, galanin R receptor (GALR) 1, GALR2, and GALR3, have been identified, all belonging to the G protein-coupled receptor (GPCR) superfamily (8–10). GALR1 is distributed mainly in the CNS, including the noradrenergic locus coeruleus neurons (11), where it may mediate the hyperpolarizing effect of galanin (12). GALR3 appears to be present at low levels in a limited number of brain regions and in several peripheral tissues (13).

GALR2 is widely distributed in the CNS, dorsal root ganglia, and many peripheral tissues such as the vas deferens, prostate, uterus, ovary, stomach, and intestine (11, 14–19). The widespread distribution of GALR2 suggests that it is involved in numerous physiological events, including prolactin release, lactation, growth hormone release, feeding, emotion, memory, nociception, cellular growth, nerve regeneration, pancreatic islet function, cardiovascular tone, peripheral metabolism, and reproduction (9). It has been shown that activation of GALR2 leads to accumulation of inositol phosphate, mobilization of intracellular Ca^{2+}, and activation of a Ca^{2+}-dependent Cl^- channel via $G_{q/11}$-type G proteins (14, 17, 20, 21). In addition, GALR2 may inhibit cAMP accumulation, presumably through $G_{i/o}$-type G proteins (17, 21). Furthermore, GALR2 has been shown to stimulate mitogen-activated protein kinase via G_o-mediated signaling (21). A more recent study reported that GALR2 plays a key role in neurite outgrowth from adult sensory neurons via a PKC-dependent pathway (22). However, so far very little information has been available on the membrane distribution of the GALRs and their intracellular trafficking. The only studies on the internalization of the GALRs used fluorescein-*N*-galanin and flow cytometry (23). No optical microscopy study has been performed to date to analyze intracellular trafficking of GALRs because of the lack of adequate antibodies.

Recently, genetic fusion of proteins to fluorescent proteins such as the jellyfish GFP (24) has provided novel means to visualize the location and real-time trafficking of GPCRs in living cells (25, 26). Here, we have taken advantage of the intrinsic fluorescent properties of enhanced GFP (EGFP), which provides a high signal-to-noise ratio and stoichiometric labeling of the receptor of interest, to investigate internalization and trafficking of GALR2, using EGFP-tagged GALR2 stably expressed in PC12 cells.

Materials and Methods

Construction of the EGFP-Tagged GALR2. For construction of GALR2-EGFP, the ORF of the rat GALR2 gene was amplified by RT-PCR with a Tian one-tube RT-PCR kit (Roche, Basel) by using forward 5′-TATAAGCTTATACCATGAATGGCTCCGGCAG-3′ and reverse 5′-TATGGTACCCCACAAGCCGGATCCAGGGTTCTAC-3′ primers. *Hin*dIII and *Kpn*I were added to forward and reverse primers, respectively, to facilitate cloning into the *Hin*dIII and *Kpn*I sites of the pEGFP-N1 vector (Clontech), to give rise to a GALR2-EGFP expression vector. CC bases were added in front of the *Kpn*I site, and the 3′ end of the ORF stop codon was deleted to put GALR2 and EGFP in the same reading frame. The plasmid of interest that had the insert in the correct orientation was identified by restriction mapping and DNA sequencing.

Transient and Stable Transfection of PC12 Cells. The PC12 cells were obtained from the American Type Culture Collection and

Abbreviations: $[Ca^{2+}]_i$, intracellular Ca^{2+} concentration; EGFP, enhanced GFP; FD, fluorescence density; FDc, FD of cytoplasm; FDm, FD of membrane; GALR, galanin R receptor; GPCR, G protein-coupled receptor; MβCD, methyl-β-cyclodextrin.

‖To whom correspondence should be addressed. E-mail: zhi-qing.xu@neuro.ki.se.

© 2004 by The National Academy of Sciences of the USA

cultured in DMEM (GIBCO) supplemented with 10% horse serum (GIBCO) and 5% FBS (GIBCO) at 37°C in a 5% CO_2 incubator. Cells were transfected by using 1 μg of DNA with a Effectene Transfection Reagent kit (Qiagen, Hilden, Germany). For transient expression, cells were used for experiments 24–48 h after transfection. To generate stable transfectants, the transfected cells were selected in the presence of the antibiotic Geneticin (G418) at 800 μg/ml. Clone expression was examined initially by fluorescence microscopy, and clones for further study were selected and expanded. Transfected PC12 cells were subcultured into eight-well chamber slides (Lab-Tek) and starved for 4 h before experiments.

Analysis of GALR2-EGFP Internalization. For ligand-induced internalization studies, the cells were treated with galanin (1×10^{-7} M) for 5, 10, 15, or 30 min at 37°C unless otherwise indicated. Some cells were coincubated with galanin (1×10^{-7} M) and Texas red-transferrin (20 μg/ml) for 30 min at 37°C. Then the cells were fixed with 10% formalin for 20 min at 4°C. Images were acquired by using a laser scanning confocal system installed on a Nikon E-600 microscope (Bio-Rad Radiance Plus) with a 63 $\times$ 1.40 oil immersion objective (Nikon). EGFP was excited with a 488-nm argon laser and detected with a 530- to 560-nm band pass filter. The Texas red-transferrin was excited at 543 nm and detected with a long pass band filter at 570 nm. For dual-color analysis, images were collected separately in single-channel mode and processed by using PHOTOSHOP (Adobe Systems, San Jose, CA). For quantification of EGFP fluorescence, digital image analysis was performed to measure the subcellular distribution of the GALR2-EGFP, using the National Institutes of Health IMAGE program (version 1.6). Thus the mean fluorescence density (FD) of EGFP of whole cell body, cytoplasm (FDc), and nucleus were measured, and data were transferred into EXCEL (Microsoft). The FD of EGFP of membrane (FDm) and FDm/FDc ratio were calculated for each cell with EXCEL.

Intracellular Ca^{2+} Concentration $[Ca^{2+}]_i$ Measurements. The cells were seeded in 0.2 ml of assay medium per well in a 96-well plate and preincubated at 5% CO_2, 37°C for 24 h. The cell plates were washed twice with preheated loading buffer (15 mM Hanks' balanced salt solution/25 mM Hepes/2.5 mM probenicid), and Fluo-4 solution was added (100 μl per well). The measurements were performed in a Fluoroscan Ascent Spectrofluorimeter (Labsystems, Hants, U.K.) with the plate chamber at 37°C and started after a 5-min equilibration period. The excitation wavelength was set to 488 nm with an emission wavelength of 535 nM. Fifteen background readings were recorded followed by addition of galanin and 30 additional readings. The fluorescence response for each well tested was calculated in activity base (IDBS), an EXCEL-based result calculation program, by importing the 16 raw data files generated for each run.

Fluorescence Correlation Spectroscopy. Fluorescence correlation spectroscopy was performed with confocal illumination of a laser volume element of 0.2 femtoliter (fl) in a ConfoCor instrument (Zeiss-Evotec) (27). As focusing optics, a Zeiss Neofluar $\times$40 numerical aperture 1.2 objective for water immersion was used in an epi-illumination setup. Separation of exciting from emitted radiation was achieved by dichroic (Omega 540 DRL PO_2, Omega Optical, Brattleboro, VT) and bandpass (Omega 565 DR 50) filters. EGFP was excited with the 488-nm line of an argon laser. Intensity fluctuations were detected by an avalanche photo diode (SPCM 200, EG & G, Vaudreuil, Quebec) and processed with a digital correlator (ALV 5000, ALV, Langen, Germany). Measurements were performed on cells cultured in 8-well Nunc chambers at 20°C. With the objective used, a 0.2-fl volume element was illuminated with dimensions of $w = 0.25$ μm and $z = 1.25$ μm, respectively.

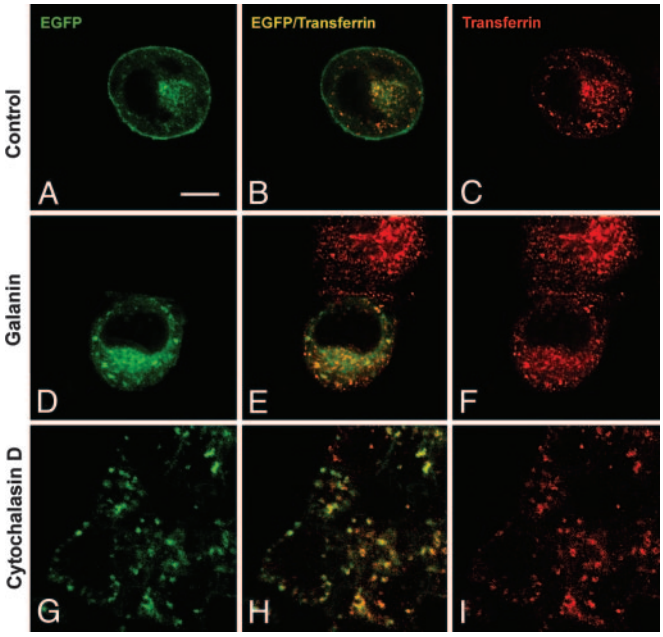

Fig. 1. Colocalization of GALR2-EGFP with transferrin. Transfected cells were incubated with Texas red-transferrin alone for 30 min (*A–C*), plus galanin (*D–F*), or plus cytochalasin D (*G–I*). The distribution of GALR2-EGFP (green) and transferrin (red) was examined with a confocal microscope. Colocalization of GALR2-EGFP with transferrin (yellow) can be observed in the merged images. (Scale bar: 8 μm.)

Results

Subcellular Distribution of GALR2-EGFP in Transfected Cells. After expression of GALR2-EGFP cDNA in PC12 cells followed by fixation and imaging in the confocal microscope, a strong green fluorescent signal was observed, whereby GALR2-EGFP predominantly appeared on the plasma membrane with some intracellular fluorescence localized mostly in presumable vesicles in the perinuclear region (Fig. 1*A*). The ratio of FDm/FDc was 1.81 ± 0.07 ($n = 20$, Fig. 2*C*). No fluorescence was detected in nontransfected PC12 cells (data not shown).

Functional Activity of GALR2–EGFP. To determine whether the GALR2-EGFP conjugate is functional and capable of coupling to the phosphatidylinositol hydrolysis signaling pathway (17, 20), PC12 cells stably expressing GALR2-EGFP were treated with galanin, and $[Ca^{2+}]_i$ was measured. Galanin caused a concentration-dependent increase in $[Ca^{2+}]_i$ levels in GALR2-EGFP-transfected cells but not in untransfected cells with an EC_{50} at 25 nM (Fig. 2*B*). Application of AR-M1986, a selective GALR2 agonist (28), induced a similar increase of $[Ca^{2+}]_i$ (data not shown). Taken together, these results show that GALR2-EGFP conjugate is functional.

Constitutively Endocytosis of GALR2-EGFP. To define the primary source of intracellular GALR2-EGFP, the distribution of GALR2-EGFP was monitored after continuous treatment (1, 2, and 4 h) with cycloheximide (25 μM), an inhibitor of protein synthesis. This treatment did not change the distribution of GALR2-EGFP (Fig. 3*B*), suggesting that the intracellular localization of GALR2-EGFP is caused by constitutive internalization and not by intracellular accumulation of newly synthesized protein. Moreover, when GALR2-EGFP-transfected cells were incubated with Texas red-conjugated transferrin, a marker for

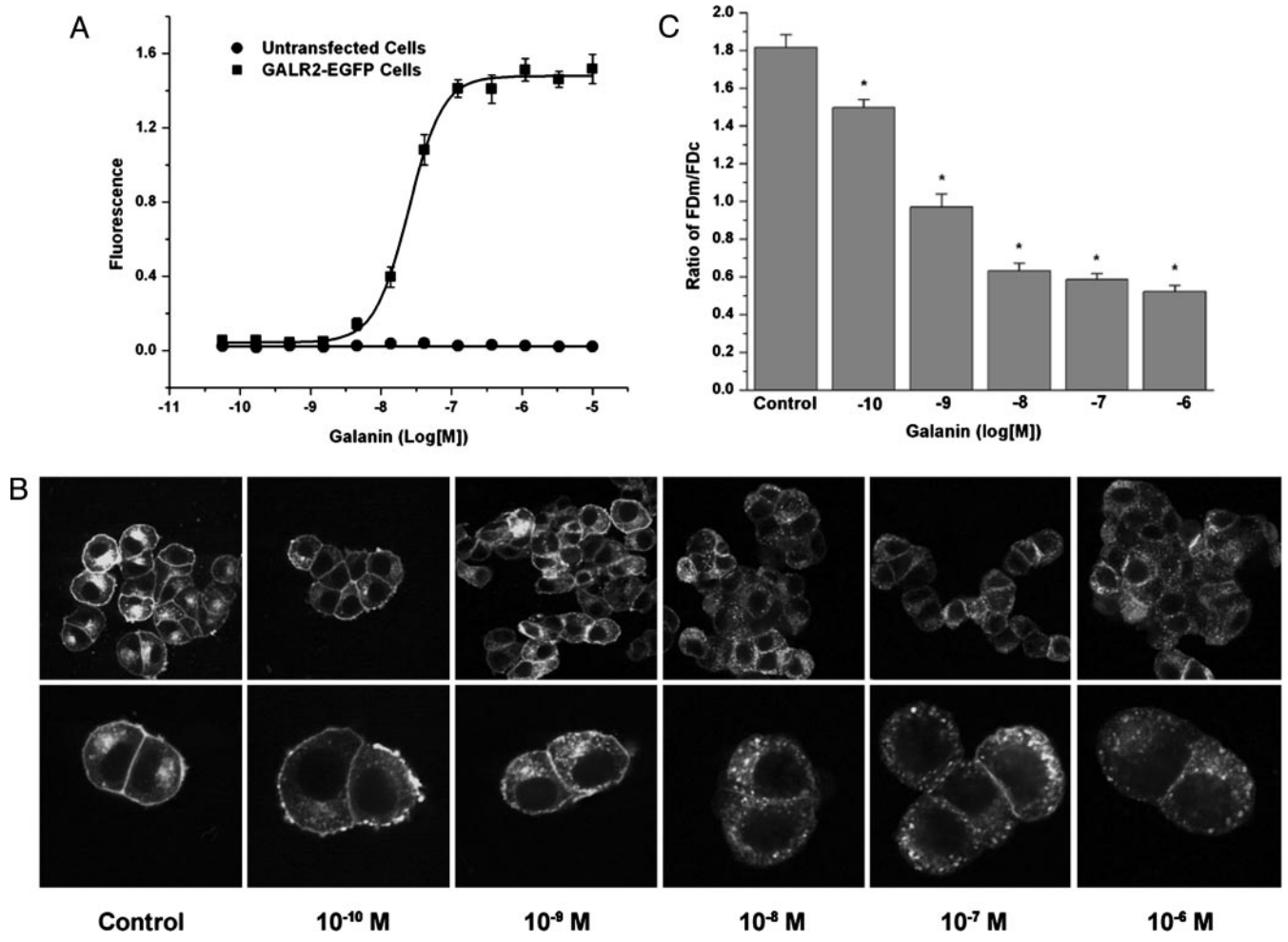

Fig. 2. Dose-dependent effect of galanin on GALR2-EGFP-transfected PC12 cells. (*A*) Galanin-induced increase in $[Ca^{2+}]_i$ levels in PC12 cells stably expressing GALR2-EGFP. Cells were treated with increasing concentrations of galanin, and $[Ca^{2+}]_i$ was monitored. The galanin-induced increase of $[Ca^{2+}]_i$ levels in transfected cells is dose-dependent with an $EC_{50} = 25$ nM. (*B* and *C*) Dose-dependent, galanin-induced internalization of GALR2-EGFP on transfected PC12 cells. Cells were treated for 30 min at 37°C with increasing concentrations of galanin and examined with confocal microscopy (*B Upper*, × 1,800; *B Lower*, × 600). (*C*) The images were quantified, and the corresponding FDm/FDc ratio was calculated in each case ($n = 20$). Results are expressed as mean ± SEM. Asterisks indicate significant difference from control ($P < 0.001$).

early and recycling endosomes (29, 30), a substantial proportion of intracellular GALR2-EGFP colocalized with transferrin (Fig. 1*B*), suggesting that intracellular GALR2-EGFP is localized to early and recycling endosomes and thus of endocytic origin. To further examine a possible constitutive internalization, we blocked endocytosis with methyl-β-cyclodextrin (MβCD) (10 mM), which inhibits clathrin-mediated endocytosis but does not affect intracellular receptor recycling and steady-state distribution of clathrin (31). After incubation with MβCD for 1 h, there appeared to be an increased amount of GALR2-EGFP on the surface and a concomitant decrease in intracellular GALR2-EGFP (Fig. 3*C*). The FDm/FDc ratio was increased to 3.44 ± 0.12 ($n = 20$) (Fig. 3*E*), indicating that the formation of the intracellular pool of receptors is a result of constitutive endocytosis. After blocking endocytic recycling for 1 h with monensin (50 μM), a potent inhibitor of recycling (32, 33), GALR2-EGFP accumulated in intracellular vesicles and decreased on the plasma membrane (Fig. 3*D*). The FDm/FDc ratio was decreased to 0.86 ± 0.06 ($n = 20$) (Fig. 3*E*). Application of cytochalasin D (4 μg/ml), which inhibits recycling by blocking actin polymerization (34, 35), also increased intracellular accumulation and decreased membrane expression of GALR2-EGFP (FDm/FDc ratio 0.83 ± 0.04, $n = 20$) (Figs. 1 *G–I* and 3*E*). Taken together, these results provide strong evidence for constitutive endocytosis of GALR2.

Endocytosis of GALR2-EGFP in Transfected PC12 Cells in Response to Galanin and Some Analogues. Incubation of GALR2-EGFP-transfected cells with galanin resulted in a dramatic redistribution of GALR2-EGFP fluorescence from the plasma membrane to an intracellular compartment, leading to a rapid and extensive decrease in surface GALR2-EGFP and with a multitude of punctate structures appearing in the cytoplasm (Fig. 1*D*) in a dose-dependent manner (Fig. 2 *B* and *C*). The FDm/FDc ratio was 1.82 ± 0.07 ($n = 20$) (Fig. 3*E*) in the absence of the ligand and decreased to 0.52 + 0.03 ($n = 20$) (Fig. 3*E*) after stimulation with galanin (10^{-6} M). Internalization was detectable after 3–5 min (Fig. 4*B*), but appeared maximal at 10–15 min (Fig. 4 *C* and *D*) and was maintained up to at least 30 min. After removal of galanin (washout), GALR2-EGFP was again seen on the plasma membrane, even in the presence of cycloheximide (Fig. 4*E*). The reinsertion of GALR2 after washout was blocked by cytochalasin D (data not shown). Restimulation with galanin after washout induced reinternalization of GALR2-EGFP (Fig. 4*F*). Application of the GALR2 agonist AR-M1986 also caused internalization of GALR2-EGFP from the plasma membrane to

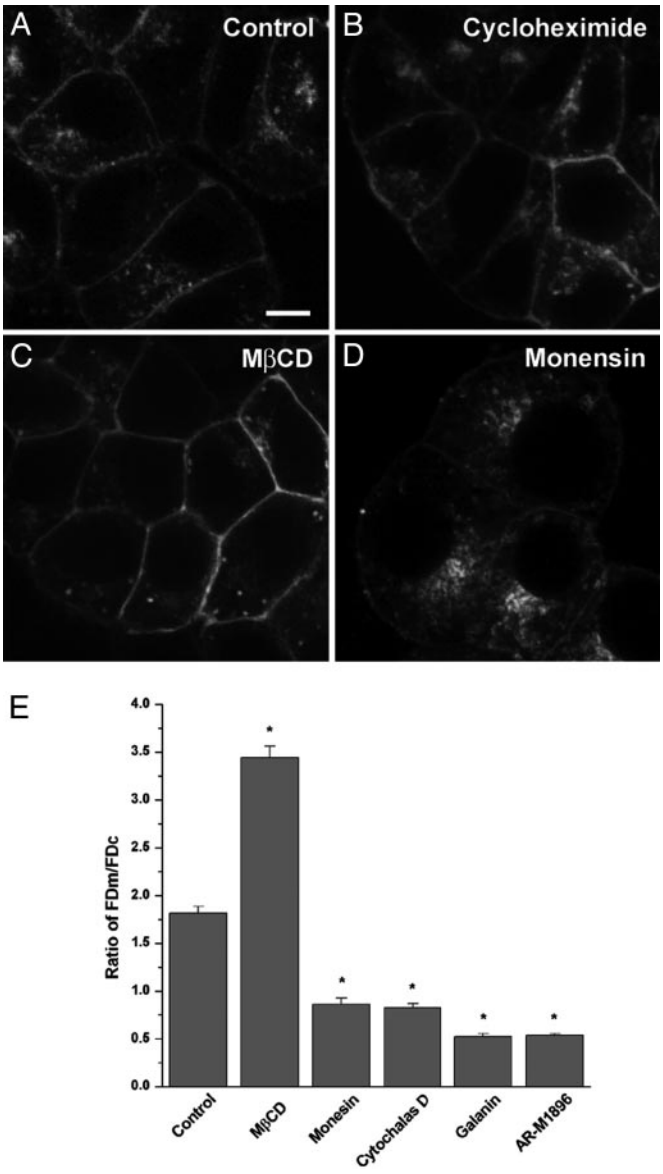

Fig. 3. Effect of monensin, MβCD, cycloheximide, galanin, and AR-M1896 on subcellular distribution of GALR2-EGFP in transfected PC12 cells. Cells transfected with GALR2-EGFP were incubated with cycloheximide (25 μM) for 4 h (*B*) or MβCD (10 mM) (*C*) or monensin (50 μM) for 1 h (*D*) at 37°C. (Scale bar: 8 μm.) (*E*) Transfected cells were examined with confocal microscopy after treatment with MβCD (10 mM), monesin (50 μM), cytochalasin D (4 μg/ml), galanin (1 μM), or AR-M1896 (1 μM). Confocal images were collected and quantified, and the corresponding FDm/FDc ratio was calculated in each case ($n = 20$). Results are expressed as mean ± SEM. Asterisks indicate significant difference from control ($P < 0.001$).

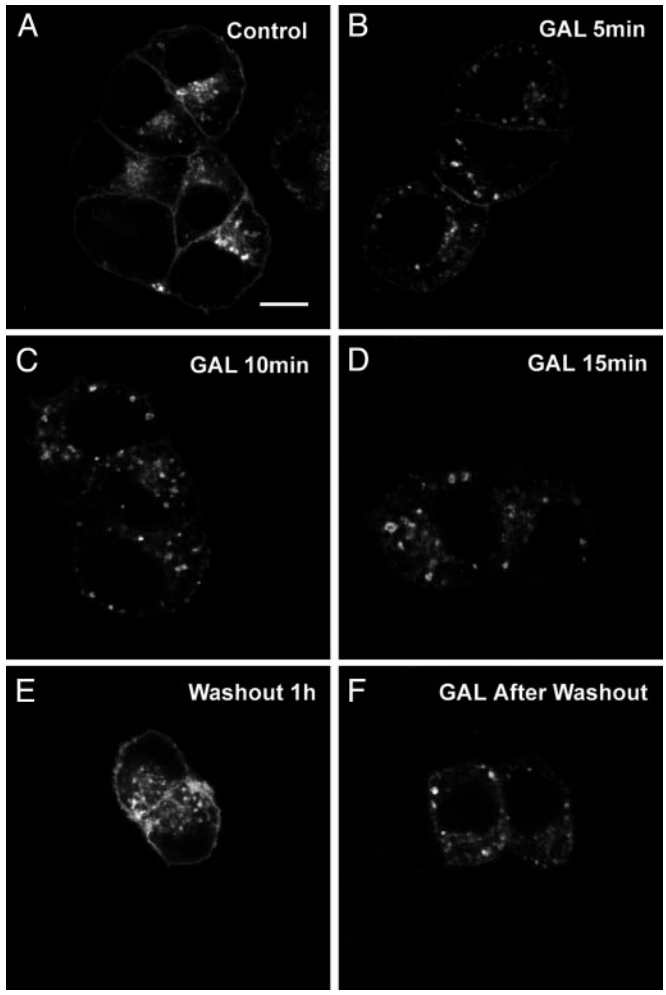

Fig. 4. GALR2-EGFP is internalized after galanin treatment and restored to the plasma membrane after washout. Internalization is detectable after 3–5 min (*B*) but appears maximal at 10–15 min (*C* and *D*). (*E*) After removal of galanin, the GALR2-EGFP is again seen on the plasma membrane. (*F*) Restimulation by galanin induces reinternalization of GALR2-EGFP. (Scale bar: 5 μm.)

the cytoplasm (Fig. 5*B*). Preincubation with the putative galanin antagonists (36) M35 (10^{-6} M) (Fig. 5*C*) or M40 (10^{-6} M) (Fig. 5*D*) induced internalization of GALR2-EGFP by themselves and did not prevent either AR-M1986- or galanin-induced internalization of GALR2-EGFP (data not shown). Both M35 and M40 also increased $[Ca^{2+}]_i$ levels in GALR2-EGFP-transfected cells (data not shown).

GALR2-EGFP Internalization Studied by Fluorescence Correlation Spectroscopy. The intensity autocorrelation function $G(\tau)$ of EGFP alone shows a diffusion time (τ_D) of 0.110 ms, which corresponds to free EGFP. The cells expressing GALR2-EGFP had the diffusion times $\tau_{D1} = 1.95$ ms and $\tau_{D2} = 60.94$ ms. Both of these diffusion times are much longer than that of free EGFP ($\tau_D = 0.110$), indicating slow diffusion of GALR2-EGFP in cells. This is also seen in the graph as a shift of the curve to the right (see Fig. 6, which is published as supporting information on the PNAS web site). Clustering/internalization of GALR2-EGFP was also examined by incubation of cells with galanin for 5 and 15 min, showing the following diffusion times: for 5 min, $\tau_{D1} = 3.81$ ms and $\tau_{D2} = 1{,}092$ ms; for 15 min, $\tau_{D1} = 5.89$ ms and $\tau_{D2} = 1{,}872$ ms. Both diffusion times are much longer than those seen in nonstimulated cells, reflecting clustering/internalization of GALR2-EGFP complexes induced by galanin stimulation. Moreover, the data also demonstrate that the clusterization/internalization increases with time. These results are in line with data in the confocal imaging studies.

Trafficking of the Endocytosed GALR2-EGFP. When transfected cells were treated with Texas red-transferrin alone, GALR2-EGFP and Texas red-transferrin were separately compartmentalized at the membrane level, not in the perinuclear area. Thus, GALR2-EGFP was located on the plasma membrane, whereas transferrin was distributed in the cytoplasm (Fig. 1 *A–C*). However, after coincubation for 30 min, the distribution of internalized

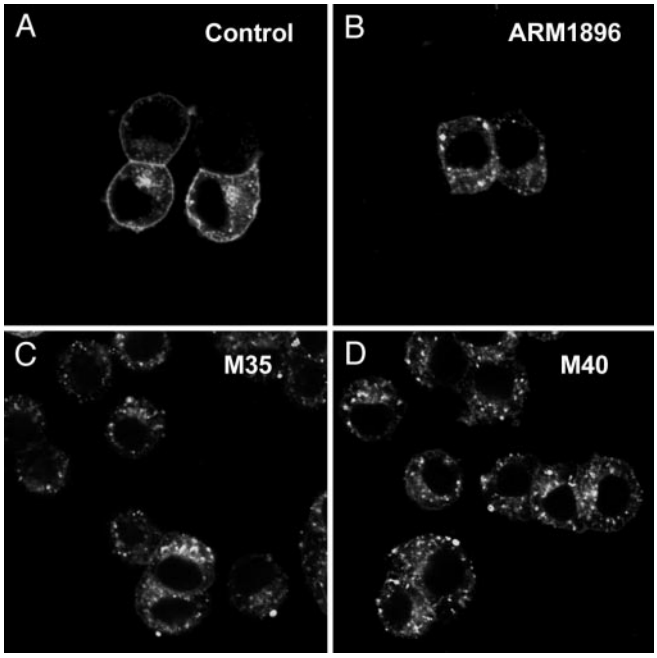

Fig. 5. Effect of galanin agonists and antagonists on GALR2-EGFP-transfected PC12 cells. (*A*) AR-M1896, a GALR2-selective agonist, induces GALR2-EGFP internalization. (*B*) Application of AR-M1986 causes internalization of GALR2-EGFP from the plasma membrane to the cytoplasm. The putative antagonists M35 (*C*) and M40 (*D*) induced internalization of GALR2-EGFP by themselves.

GALR2-EGFP and Texas red transferring overlapped strongly (Fig. 1 *D–F*). After treatment with 0.4 M sucrose for 5 min before coincubation, internalization of GALR2-EGFP did not occur (data not shown). However, GALR2-EGFP was distributed nonuniformly along the plasma membrane as puncta/clusters (data not shown). After incubation with galanin at 4°C, GALR2-EGFP was aggregated and clustered on the membrane, but not distributed to the deeper cytoplasm as was the case at 37°C (data not shown).

Discussion

The present study was undertaken to address membrane expression, trafficking, and internalization of GALR2 by stably expressing this receptor fused with EGFP in PC12 cells. We provide evidence here that GALR2 displays a significant level of ligand-independent, i.e., constitutive internalization. Our study also demonstrates that ligand-induced internalization of GALR2 uses the clathrin-dependent, endocytic recycling pathway.

GALR1 is mainly distributed to the CNS and dorsal root ganglia, and GALR3 is present only at low levels in brain but more extensively in several peripheral tissues, GalR2 mRNA is abundantly expressed in the CNS, including hippocampus, and in many peripheral tissues (11, 14–19). However, because of the lack of specific antibodies against GALR2, many aspects of its distribution and trafficking have so far not been characterized. Using a stably expressed GALR2-EGFP fusion protein we are now able to directly examine the subcellular localization of GALR2 and its intracellular trafficking at steady state or upon ligand stimulation. Using confocal fluorescence microscopy the fusion protein was visualized in transfected PC12 cells with a predominantly plasma membrane localization. It has been demonstrated that GalR2 is coupled to $G_{q/11}$, leading to inositol phosphate accumulation and calcium mobilization (17, 20). Indeed, in the present study, application of galanin and the GALR2 agonist AR-M1986 induced a concentration-dependent increase in $[Ca^{2+}]_i$ levels in GALR2-EGFP-transfected, but not in control PC12 cells, indicating that the GALR2-EGFP conjugate is functional and still maintains the pharmacological and signal transduction properties even after fusion with the large protein EGFP to its C terminal.

The question of intracellular trafficking of constitutively active WT GPCRs has recently become of increasing interest, since it was first reported for the δ-opioid receptor (37). Thus, the chemokine CXCR4 receptor (38), thyrotropin receptor (32), M2 muscarinic receptor (39), thrombin receptor (40), human cytomegalovirus chemokine receptor (41), and cannabinoid type receptor (42) all have been observed undergoing constitutive endocytosis in the absence of ligand. The constitutive internalization of a given GPCR might be important for maintenance of cellular homeostasis and could have a direct impact on the potency of agonists in receptor-mediated signaling by altering surface density of a receptor. The present data also suggest that GALR2 undergoes constitutive endocytosis. Thus, at steady-state GALR2-EGFP is expressed on the plasma membrane, but a substantial proportion of receptors is also present in intracellular vesicles. Intracellular-located GALR2-EGFP is not affected by protein synthesis inhibition by cycloheximide. Transferrin is endocytosed together with cell-surface transferrin receptors and then selectively sorted into early and recycling endosomes. It represents an established marker for this type of endosomes (29, 30) and has been extensively used for studies of the recycling pathway. In the present study, after incubation with Texas red-transferrin, but without ligand stimulation, GALR2-EGFP appeared in intracellular vesicles containing transferrin, indicating that GALR2 undergoes constitutive endocytosis and recycling. Inhibition of clathrin-mediated endocytosis by acute depletion of plasma membrane cholesterol with MβCD (30) increased the FDm/FDc ratio, i.e., enhanced expression of GALR2 on the plasma membrane and decreased intracellular accumulation of GALR2, demonstrating that clathrin-mediated endocytosis is involved in the generation of the intracellular population of GALR2. Two recycling inhibitors, monensin and cytochalasin D (32–35), were applied, and both of them caused reduction of membrane expression of GALR2-EGFP and enhanced accumulation of GALR2-EGFP in cytoplasm, further supporting the role of recycling in maintaining GALR2-EGFP surface level.

Persistent stimulation of GPCRs often leads to internalization of receptor proteins into intracellular vesicles (43, 44). This endocytic process has been shown to be regulated mainly by two families of key proteins, the GPCR kinase and the β-arrestins (45, 46). In general, such ligand-induced endocytosis contributes to the physiological regulation of a wide variety of signaling receptors, whereby the desensitization phenomenon plays a particularly important role (47). Using a fluorescein-*N*-galanin and flow cytometry, ligand-induced internalization of GALR1 has been reported in transfected Chinese hamster ovary cells (23). In the present study, upon agonist challenge by galanin, GALR2-EGFP was internalized in a time- and dose-dependent manner. Moreover, application of AR-M1986 induced internalization of GALR2-EGFP but not GALR1-EGFP (S.X, T.H., and Z.-Q.D.X, unpublished data), confirming that AR-M1986 is a selective agonist for GALR2 (28). A series of chimeric peptides using the NH2-terminal GAL-(1–12) fragment and a COOH-terminal portion of another bioactive or nonsense peptide have been synthesized (36). In particular, two of these compounds, M35 and M40, have been shown to act as functional antagonists in several experimental models (48). In the present study, neither M35 nor M40 prevented internalization of GALR2-EGFP. On the contrary, both M35 and M40 elicited internalization and an increase in $[Ca^{2+}]_i$ levels by themselves, suggesting that they act as GALR2 agonists. Our results support earlier studies that

these putative galanin antagonists possess agonist properties of GALR2s (14, 17, 18, 20).

With fluorescence correlation spectroscopy (27), we observed that the diffusion times after both 5 and 17 min of agonist application were much longer than in nonstimulated cells, corresponding to clustered/internalized complexes of GALR2, in line with our data from the confocal imaging studies.

Upon galanin challenge, GALR2-EGFP was internalized and reinserted after washout, suggesting that GALR2s are recycled back to the cell surface. Because cycloheximide was used to prevent protein neosynthesis and did not inhibit receptor recycling to the cell surface, we conclude that synthesis of new protein is not involved in the recycling process. Internalized GALR2-EGFP was extensively colocalized with Texas red-transferrin. As transferrin is a marker of the clathrin endocytic pathway (29, 30), GALR2 appears to use the same pathway. This idea was further supported by showing that GALR2-EGFP failed to be endocytosed in the presence of 0.4 M sucrose, which is known to perturb clathrin-coated pit formation, i.e., block internalization processes that use clathrin-coated pits and vesicles (49, 50). Stimulation of galanin at low temperature caused aggregation and clustering of GALR2-EGFP on the surface but no transport to deep cytoplasm. This finding suggests that intracellular vesicular trafficking of GALR2-EGFP is a temperature-dependent process. It has been reported that interaction of the receptor's cytoplasmic internalization signal with the clathrin adaptor protein AP2 is temperature-sensitive (51), providing further support that the clathrin pathway is involved in GALR2 endocytosis.

We thank Professor Tamas Bartfai (The Scripps Research Institute, La Jolla, CA) and Dr. Madis Metsis (Center for Genomics and Bioinformatics, Karolinska Institutet) for valuable support and Dr. Ralf Schmidt (AstraZeneca R&D, Montreal) for the generous supply of AR-M1896. This study was supported by Swedish Science Council Grant 04X-2887, European Community Grant NEWMOOD-LSHMK-CT-2003-503474, The Marianne and Marcus Wallenberg Foundation, The Knut and Alice Wallenberg Foundation, The Harald and Greta Jeansson Foundation, Svenska Läkaresällskapet, The Alzheimer Foundation, Stiftelsen Lars Hiertas Minne and Karolinska Institutet, and an unrestricted Bristol-Myers Squibb Neuroscience Grant. S.X. is supported by an International Brain Research Organization Fellowship and a European Molecular Biology Organization Fellowship.

1. Tatemoto, K., Rokaeus, A., Jornvall, H., McDonald, T. J. & Mutt, V. (1983) *FEBS Lett.* **164,** 124–128.
2. Hökfelt, T., Bartfai, T. & Crawley, J. eds. (1998) *Ann. N.Y. Acad. Sci.* **863,** 1–469**.**
3. Wynick, D. & Bacon, A. (2002) *Neuropeptides* **36,** 132–144.
4. Seutin, V., Verbanck, P., Massotte, L. & Dresse, A. (1989) *Eur. J. Pharmacol.* **164,** 373–376.
5. Sevcik, J., Finta, E. P. & Illes, P. (1993) *Eur. J. Pharmacol.* **230,** 223–230.
6. Pieribone, V., Xu, Z.-Q., D., Zhang, X., Grillner, S., Bartfai, T. & Hökfelt, T. (1994) *Neuroscience* **6,** 861–874.
7. Xu, Z.-Q. D., Zhang, X., Pieribone, V. A., Grillner, S. & Hökfelt, T. (1998b) *Neuroscience* **87,** 79–94.
8. Habert-Ortoli, E., Amiranoff, B., Loquet, I., Laburthe, M. & Mayaux, J.-F. (1994) *Proc. Natl. Acad. Sci. USA* **91,** 9780–9783.
9. Iismaa, T. P. & Shine, J. (1999) *Results Probl. Cell Differ.* **26,** 257–291.
10. Branchek, T. A., Smith, K. E., Gerald, C. & Walker, M. W. (2000) *Trends Pharmacol. Sci.* **21,** 109–117.
11. O'Donnell, D., Ahmad, S., Wahlestedt, C. & Walker, P. (1999) *J. Comp. Neurol.* **409,** 469–481.
12. Ma, X., Tong, Y. G., Schmidt, R., Brown, W., Payza, K., Hodzic, L., Pou, C., Godbout, C., Hökfelt, T. & Xu, Z.-Q. D. (2001) *Brain Res.* **919,** 169–174.
13. Mennicken, F., Hoffert, C., Pelletier, M., Ahmad, S. & O'Donnell, D. (2002) *J. Chem. Neuroanat.* **24,** 257–268.
14. Fathi, Z., Cunningham, A. M., Iben, L. G., Battaglino, P. B., Ward, S. A., Nichol, K. A., Pine, K. A., Wang, J., Goldstein, M. E., Iismaa, T. P., *et al.* (1997) *Brain Res. Mol. Brain Res.* **51,** 49–59.
15. Howard, A. D., Tan, C., Shiao, L. L., Palyha, O. C., McKee, K. K., Weinberg, D. H., Feighner, S. D., Cascieri, M. A., Smith, R. G., Van Der Ploeg, L. H., *et al.* (1997) *FEBS Lett.* **405,** 285–290.
16. Shi, T. J., Zhang, X., Holmberg, K., Xu, Z.-Q. D. & Hökfelt, T. (1997) *Neurosci. Lett.* **237,** 57–60.
17. Smith, K. E., Forray, C., Walker, M. W., Jones, K. A., Tamm, J. A., Bard, J., Branchek, T. A., Linemeyer, D. L. & Gerald, C. (1997) *J. Biol. Chem.* **272,** 24612–24616.
18. Wang, S., Hashemi, T., He, C., Strader, C. & Bayne, M. (1997) *Mol. Pharmacol.* **52,** 337–343.
19. Xu, Z.-Q. D., Shi, T.-J. S. & Hökfelt, T. (1998) *J. Comp. Neurol.* **392,** 227–252.
20. Fathi, Z., Battaglino, P. M., Iben, L. G., Li, H., Baker, E., Zhang, D., McGovern, R., Mahle, C. D., Sutherland, G. R., Iismaa, T. P., *et al.* (1998) *Brain Res. Mol. Brain Res.* **58,** 156–169.
21. Wang, S., Hashemi, T., Fried, S., Clemmons, A. L. & Hawes, B. E. (1998) *Biochemistry* **37,** 6711–6717.
22. Mahoney, S. A., Hosking, R., Farrant, S., Holmes, F. E., Jacoby, A. S., Shine, J., Iismaa, T. P., Scott, M. K., Schmidt, R. & Wynick, D. (2003) *J. Neurosci.* **23,** 416–421.
23. Wang, S., Clemmons, A., Strader, C. & Bayne, M. (1998) *Biochemistry* **37,** 9528–9535.
24. Kaether, C. & Gerdes, H. H. (1995) *FEBS Lett.* 369267–369271.
25. Tsien, R. Y. (1998) *Annu. Rev. Biochem.* **67,** 509–544.
26. Kallal, L. & Benovic, J. L. (2000) *Trends Pharmacol. Sci.* **21,** 175–180.
27. Rigler, R. (1995) *J. Biotechnol.* **41,** 177–186.
28. Liu, H. X., Brumovsky, P., Schmidt, R., Brown, W., Payza, K., Hodzic, L., Pou, C., Godbout, C. & Hökfelt, T. (2001) *Proc. Natl. Acad. Sci. USA* **98,** 9960–9964.
29. Woods, J. W., Goodhouse, J. & Farquhar, M. G. (1989) *Eur. J. Cell Biol.* **50,** 132–143.
30. von Zastrow, M. & Kobilka, B. K. (1992) *J. Biol. Chem.* **267,** 3530–3538.
31. Subtil, A., Gaidarov, I., Kobylarz, K., Lampson, M. A., Keen, J. H. & McGraw, T. E. (1999) *Proc. Natl. Acad. Sci. USA* **96,** 6775–6780.
32. Baratti-Elbaz, C., Ghinea, N., Lahuna, O., Loosfelt, H., Pichon, C. & Milgrom, E. (1999) *Mol. Endocrinol.* **13,** 1751–1765.
33. Miserey-Lenkei, S., Parnot, C., Bardin, S., Corvol, P. & Clauser, E. (2002) *J. Biol. Chem.* **277,** 5891–5901.
34. Durrbach, A., Louvard, D. & Coudrier, E. (1996) *J. Cell. Sci.* **109,** 457–465.
35. Bartz, R., Benzing, C. & Ullrich, O. (2003) *Biochem. Biophys. Res. Commun.* **312,** 663–669.
36. Bartfai, T., Fisone, G. & Langel, U. (1992) *Trends Pharmacol. Sci.* **13,** 312–317.
37. Costa, T. & Herz, A. (1989) *Proc. Natl. Acad. Sci. USA* **86,** 7321–7325.
38. Signoret, N., Oldridge, J., Pelchen-Matthews, A., Klasse, P. J., Tran, T., Brass, L. F., Rosenkilde, M. M., Schwartz, T. W., Holmes, W., Dallas, W., *et al.* (1998) *J. Cell Biol.* **139,** 651–664.
39. Roseberry, A. G. & Hosey, M. M. (1999) *J. Biol. Chem.* **274,** 33671–33676.
40. Shapiro, M. J., Trejo, J., Zeng, D. & Coughlin, S. R. (1996) *J. Biol. Chem.* **271,** 32874–32880.
41. Fraile-Ramos, A., Kledal, T. N., Pelchen-Matthews, A., Bowers, K., Schwartz, T. W. & Marsh, M. (2001) *Mol. Biol. Cell* **12,** 1737–1749.
42. Leterrier, C., Bonnard, D., Carrel, D., Rossier, J. & Lenkei, Z. (2004) *J. Biol. Chem.* **279,** 36013–36021.
43. Sibley, D. R., Benovic, J. L., Caron, M. G. & Lefkowitz, R. J. (1987) *Cell* **48,** 913–922.
44. von Zastrow, M. (2001) *Biochem. Soc. Trans.* **29,** 500–504.
45. Claing, A., Laporte, S. A., Caron, M. G. & Lefkowitz, R. J. (2002) *Prog. Neurobiol.* **66,** 61–79.
46. Shenoy, S. K. & Lefkowitz, R. J. (2003) *Biochem. J.* **375,** 503–515.
47. Ferguson, S. S. (2001) *Pharmacol. Rev.* **53,** 1–24.
48. Langel, Ü. & Bartfai, T. (1998) *Ann. N.Y. Acad. Sci.* **863,** 86–93.
49. Daukas, G. & Zigmond, S. H. (1985) *J. Cell Biol.* **101,** 1673–1679.
50. Heuser, J. E. & Anderson, R. G. (1989) *J. Cell Biol.* **108,** 389–400.
51. Fire, E., Brown, C. M., Roth, M. G., Henis, Y. I. & Petersen, N. O. (1997) *J. Biol. Chem.* **272,** 29538–29545.